Column Stiffness Requirements for Diagonally Stiffened Steel Plate Shear Walls

Amr A. Elbanna, Sherif S. Safar, Mokhtar M. Seddik

Abstract*: Various numerical models of diagonally stiffened steel plate shear wall were tested under push-over loads to study the required stiffness of columns of diagonally stiffened SPSWs. This research presents a parametric study to explore the influence of varying the infill panel's thickness, width, and height and the number of floors on the stiffness of the edge columns, and to propose expressions to predict the column's in-plane stiffness and area required for preliminary design. Different SPSWs were modeled with a range of several stories, an aspect ratio, and height to thickness ratio, respectively, of (n=3-7), (L_p/h_p=1-2), and (λ=200-400). The results indicated that the number of floors (n) has a great effect on the wall's shear capacity. A greater number of floors lead to buckling in columns and early failure of the system, and subsequently, an increase in the column's rigidity is required. Higher the drift is, lower the shear capacity of the wall is, particularly for walls with a larger aspect ratio ($L_p/h_p > 1.5$), and smaller height to thickness ratio ($\lambda < 400$). It is proposed that the columns' out-of-plane stiffness divided by its in-plane stiffness to be equal or greater than 0.4. Equations are proposed to predict the required columns' r_x, and ω_h substantial to assure that the columns can resist the impact of the tension field and the plate achieves full yield strength.

***Keywords:* Push-over analysis, Steel plate shear walls, Diagonally stiffened, Ultimate strength, Stiffness, Column stiffness.**

I. INTRODUCTION

One of the most economical and effective lateral loads resisting systems and retrofitting existing buildings used since the 1970s is the steel plate shear walls (SPSWs). This is due to that this lateral load resisting technique possesses several advantages (excellent post-buckling capacity, high elastic stiffness, high energy dissipation capacity, and stable hysteretic behavior). Also, buildings constructed with SPSWs exhibits lightweight compared to those constructed with conventional reinforced concrete walls. However, SPSW systems have several disadvantages, for example, it suffers from the flexural flexibility, and therefore many authors recommended to strengthen the wall either by adding stiffeners or utilizing composite concrete infill steel pipe columns at the corners of the wall. The typical stiffened SPSW composes of a thin steel plate stiffened by different configurated stiffeners and bounded by vertical elements (columns) and horizontal elements (beams). Cassese et al. (1993) [1] discussed the influence of the thickness of the plate and the connection type between beam and column on the manner and response of unstiffened SPSW. Six quarter-scale three-stories single-bay unstiffened specimens were prepared and subjected to quasi-static cyclic loads. They observed that when the plate thickness exceeded the optimum thickness they identified, the strength of SPSW was not increased, and the system fails due to column buckling or yielding. Furthermore, the beam-to-column connection displayed almost no significant effect on the manner of SPSW. Based on the previous searches, when an un-stiffened steel infill panel with a smaller height-to-thickness ratio (λ) is loaded with a higher horizontal force, tension fields are formed because of the generated large out-of-plane buckling of the plate. These greater forces resulted from the tension fields may lead to failure of the boundary elements [2-5]. Authors suggested constructing shear walls with various configurated stiffeners (cross stiffeners, diagonal stiffeners, etc.) to lessen the wall's out-of-plane deformation [6-13]. F. Nateghi and E. Alavi (2009) [14] investigated the behavior of stiffened and unstiffened steel plate shear walls under seismic loads. Push-over analysis using ANSYS was executed on a stiffened SPSW model with two-sided diagonal stiffeners of different sizes as well as an unstiffened SPSW model. It was found that as the width to thickness ratio of the diagonal stiffeners decreased, their local buckling reduced. The diagonal stiffeners decreased the buckling lengths of the inclined strips as compared to unstiffened SPSWs. The diagonally stiffened SPSW model showed higher shear strength and stiffness by about 15% and 30%, respectively, compared to the unstiffened model. Furthermore, good approval between the outcomes of the non-linear analysis and the theoretical method. M. Wang et al. (2015) [15] used analytical finite element method to study the behavior of different construction details of steel plate shear wall structures, such as load-carrying capacity, ductility, energy-dissipating capacity, out-of-plane deformations, the influence of tension field on the column and economic performance under seismic load. The results indicated that the finite element methodology is the perfect technique to study the performances of steel plate shear walls. It should be noted that SW-T-LYP, SW-SF, SW-H1, and SW-H2 specimens showed an effective decrease in out-of-plane deformation.

Revised Manuscript Received on March 30, 2020.
* Correspondence Author
Amr A. Elbanna*, Civil Engineering Department, Beni-suef University, Beni-suef, Egypt. Email: amr_elbana2020@yahoo.com
Sherif S. Safar, Civil Engineering Department, Cairo University, Giza, Egypt. Email: sherifsafar@yahoo.com
Mokhtar M. Seddik, Civil Engineering Department, Cairo University, Giza, Egypt.

SW-LYP, SW-T-LYP, SW-CF, SW-SF, SW-H1, and SW-H2 specimens achieved good ductility. SW-CF, SW-T-LYP, SW-LYP, SW-H1, and SW-H2 specimens reduced the impact of tension fields on the columns. SW-CR and SW-SR specimens showed an increase in the load-carrying capacity. SW-SF, SW-CF, SW-LYP, and SW-T-LYP achieved better energy dissipation capacity. Moreover, it appeared that T-type stiffened ribs low yield point steel plate shear wall had the better load-carrying capacity and smallest out-of-plane deformation, besides, it minimizes the impact of tension field on the columns and upgrades the energy dissipation capacity and cumulative damage.

II. VALIDATION OF FINITE ELEMENT ANALYSIS

Typical quasi-static cyclic loading tests, including Park et al. [16] and M.A. Sigariyazd et al. [13], were chosen to verify the finite element method.

A. Tests of Park et al. (2007)

Five single-bay three-story specimens divided into two series (SC and WC) were fabricated for the experimental program denoted as SC2T, SC4T, SC6T, WC4T, and WC6T. Fig. 1 represents the details of the typical specimen tested by Park et al. All these specimens are verified herein. The size of the infill panel was (1500 mm x 1000 mm x various thicknesses). The thickness of the plate of SC2T specimen is 2 mm, SC4T and WC4T is 4 mm, and SC6T and WC6T is 6 mm. As per the requirements of the Korean standard, the plate of thickness 2 mm was made of SS400, 4 mm of SM490, and 6 mm of SM490 with yield strength F_y equal to 240, 330, and 330 MPa, respectively. Built-up sections were used to manufacture the frame members. The beam used at the third story was H-400x200x16x16 mm, while the beams used at the first and second stories were H-200x200x16x16 mm. The columns used in the SC series were strong (H-250x250x20x20 mm), while those used in the WC series were weak and non-compact sections (H-250x250x9x12 mm). Fish plates of size (80 mm x 9 mm) were utilized to connect the boundary frame elements (VBE and HBE) to the steel plates. All specimens were subjected to cyclic loading with target displacements $\pm 0.2\delta_y$, $0.4\delta_y$, $0.6\delta_y$, $0.8\delta_y$, $1.0\delta_y$, $1.5\delta_y$, $2\delta_y$, $3\delta_y$, $4\delta_y$, $6\delta_y$, and $8\delta_y$. Fig. 2,3, and 4 depict the equivalent stresses and out-of-plane deformations for specimens SC4T, WC4T, and WC6T, respectively. The outcomes obtained from the experimental program are of good approval with those obtained from the numerical analysis. Fig. 5 and 6 clarify the comparison between load-displacement curves obtained from both experimental test and finite element analyses.

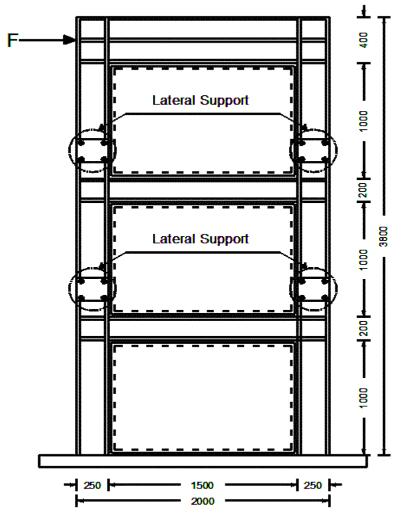

Fig. 1.Details of typical model tested by Park et al [16].

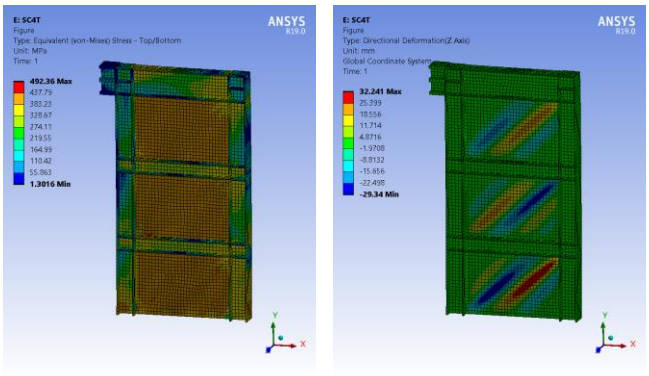

(a) Equivalent stress (b) Out-of-plane deformation

Fig. 2.Equivalent stress and out-of-plane deformation for specimen SC4T.

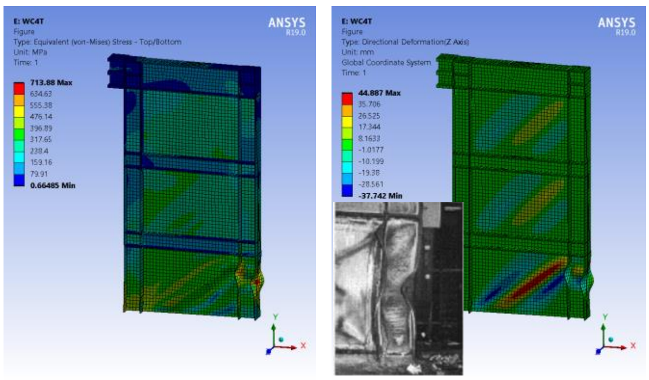

(a) Equivalent stress (b) Out-of-plane deformation

Fig. 3.Equivalent stress and out-of-plane deformation for specimen WC4T.

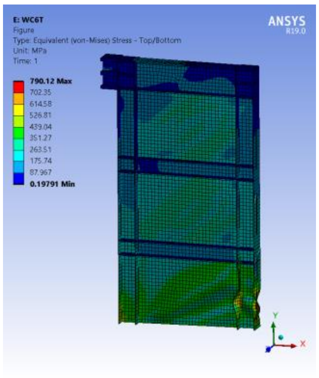

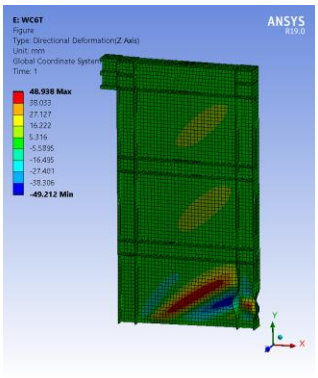

(a) Equivalent stress (b) Out-of-plane deformation

Fig. 4.Equivalent stress and out-of-plane deformation for specimen WC6T.

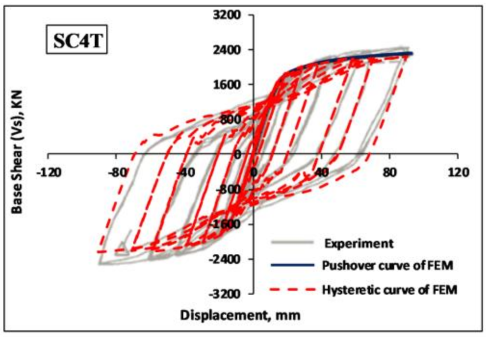

(a)

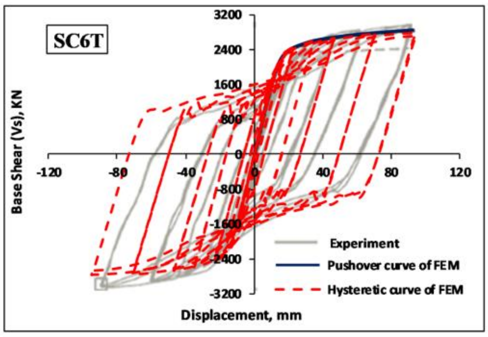

(b)

Fig. 5.Comparison of hystresis curves tested by Park et al. and FE analysis.

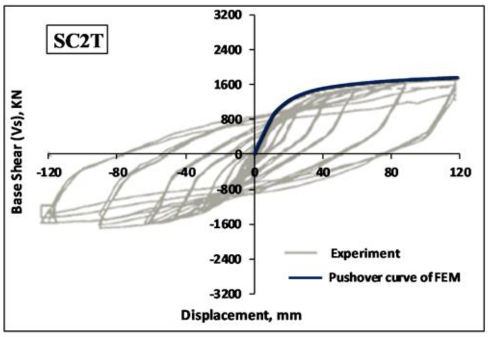

(a)

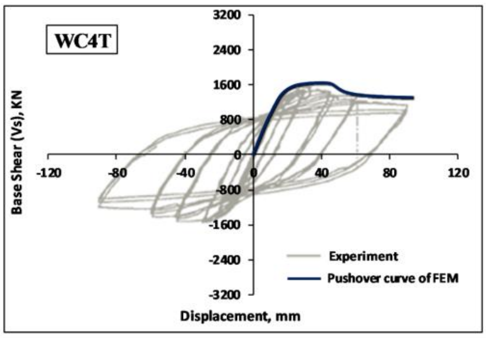

(b)

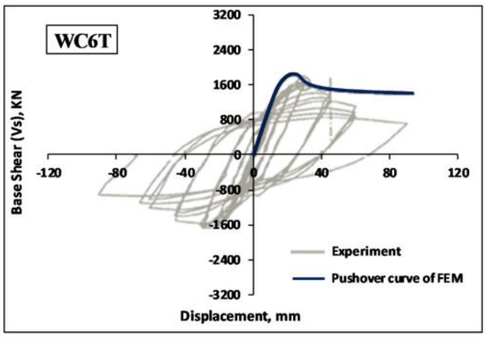

(c)

Fig. 6.Comparison of hystresis curves and numerical pushover curves tested by Park et al.

B. Tests of M.A. Sigariyazd et al. (2016).

Three single-bay single-story specimens were fabricated, and designated as SPW-0 (un-stiffened specimen), SPW-1 and SPW-2 (different configurated stiffened specimens) to assess the behavior of frame members and infill panels. Details of tested SPW-2 specimen is depicted in Fig. 7. All three specimens were selected in the validation herein. According to the DIN standard, the boundary frame and the infill panel was made of ST37 and ST12, respectively. The size of the infill panel for all the three specimens was (1160 mm x 980 mm x 1.5 mm). For SPSW-1 and SPSW-2, plates of size (40 mm x 4 mm x length) were used to fabricate the diagonal stiffeners. Both the columns and beams were built-up sections of plate elements. Lateral loads were applied at the level of the top beam by a horizontal hydraulic jack. The equivalent stress of the three tested specimens is illustrated in Fig. 8. The outcomes of the numerical analysis and the experimental tests are of good agreements. Fig. 9 illustrates the load-displacement curves obtained from numerical analysis and experimental tests.

Retrieval Number: E2249039520/2020©BEIESP
DOI: 10.35940/ijitee.E2249.039520
Journal Website: www.ijitee.org

Published By:
Blue Eyes Intelligence Engineering
& Sciences Publication

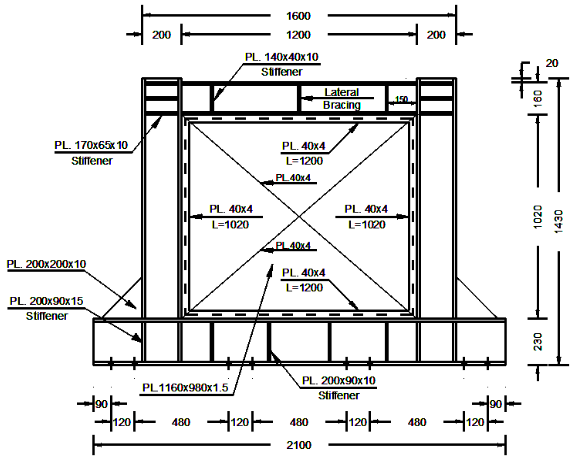

Fig. 7.Experimental model for specimen SPW-2 tested by M.A. Sigariyazd et al. [13].

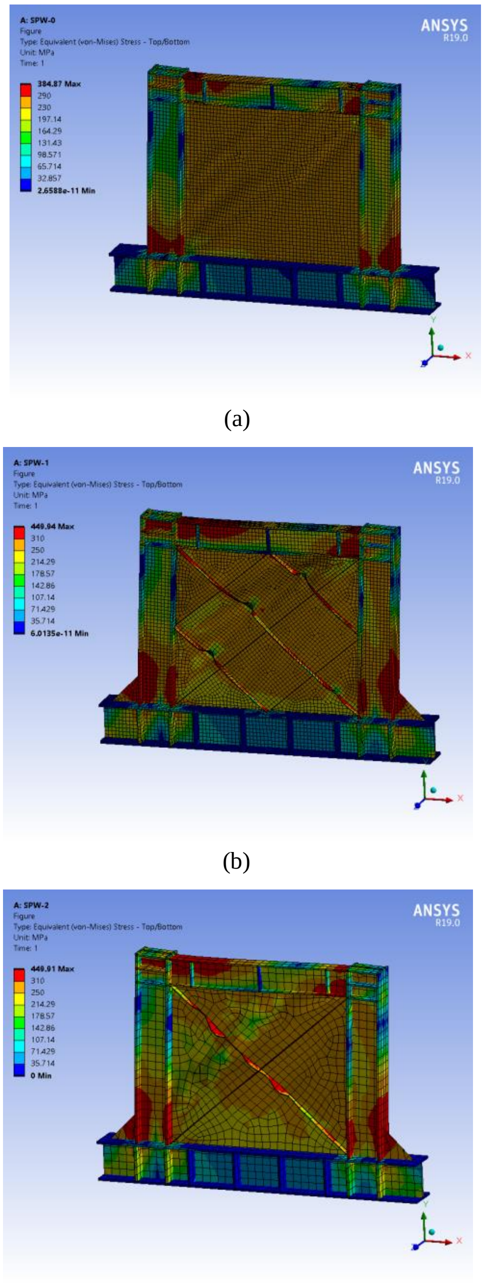

(a)

(b)

(c)

Fig. 8.Equivalent stresses of specimens tested by M.A. Sigariyazd et al. [13].

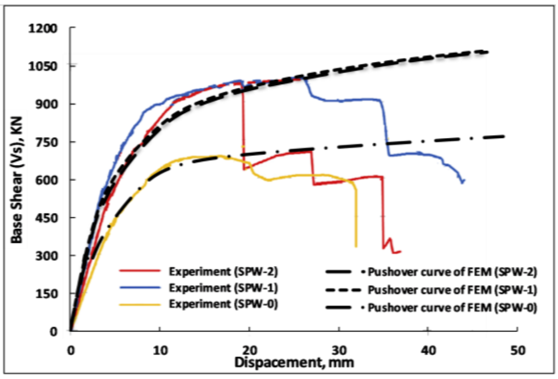

Fig. 9.Comparion of push-over curves tested by M.A. Sigariyazd et al. and FE analysis.

III. NUMERICAL MODELLING AND SIMULATION

Scholars relied on the finite element methodology in the structural analysis field to study, understand, and estimate the behavior of steel plate shear walls under lateral loads.

A. Description of finite element models

The three-dimensional finite element analysis was executed in **ANSYS** with SHELL 181 elements. In this paper, the sections of the boundary elements were selected as per both the American and Canadian codes' specifications [17,18]. The sections of the beams were the same for all models where the intermediate beam was (H300x250x20x38), and the top beam was (H500x250x38x52). The columns' in-plane stiffness I_c was obtained from Eq. (1) by considering ω_h to be within the range of 1.8-3.

$$\omega_h = 0.7h\left[\frac{t_i}{2LI_c}\right]^{0.25} \tag{1}$$

, where h is the distance measured between the centerlines of the edge beams, t_i is the thickness of the plate, and L is the distance measured between the centerlines of the edge columns.

The stiffeners' dimensions were chosen according to AISC [17], and the value of the width to thickness ratio is calculated from the following expression:

$$b_s / t_s \le 0.56\sqrt{\frac{E}{\sigma_{ys}}} \tag{2}$$

By substituting the selected values of both modulus of elasticity (E) and yield strength of stiffeners (σ_{ys}), Eq. (2) is abbreviated to ($b_s/t_s \le 12$). The infill plate's and stiffeners' yield strength were assumed to be 240 MPa, while that of the boundary elements was to be 360 MPa. The monotonic push-over loading was utilized to simulate an earthquake load. The final loading state of SPSWs was considered to occur when the displacement value on the top floor at a drift ratio reaches 3%, at least at one of the floors of the model. Fig. 10 represents the detailed dimensions of the basic model, including the dimensions of stiffeners, top beam, and intermediate beams. The fixed boundary conditions allocated at the base of the wall were created by constraint versus both rotation and translation.

The model was supported in the out-of-plane direction at the level of floor beams to ensure stability. For the best outcomes and results of the finite element analysis, the convenient mesh size was chosen by comparing the model of stiffened SPSW with element size (30x30) mm, selected as a reference, with other different element sizes. Table I shows the finite element mesh size (mm) and the corresponding average error for the element size 30mm. The mesh size used is (100x100) mm, with an error of less than 1%.

Table- I: Results of mesh sensitivity analysis

Finite element mesh size (mm)	Average error
30	-----
50	0.26
100	0.82
150	1.68
200	1.93
250	3.49
300	3.54

The initial defects were imposed by editing the inp file of the first buckling mode. Non-linear stabilization technique was accomplished by inserting the damping factor at each node [19]. The main purpose of this method is the strict convergence that happened because, of the sudden increment in the infill panel's out-of-plane displacements. The damping force generated from the damping unit is proportional to nodal displacement increment. Thereafter, any node tends to be unstable large displacement increments generated a large damping force that decreased the displacement and stabilized the system. Due to the small value of the damping force parallel to the internal force, the damping force generated less energy. As a result, the damping force has a small effect on the results of the finite element analysis.

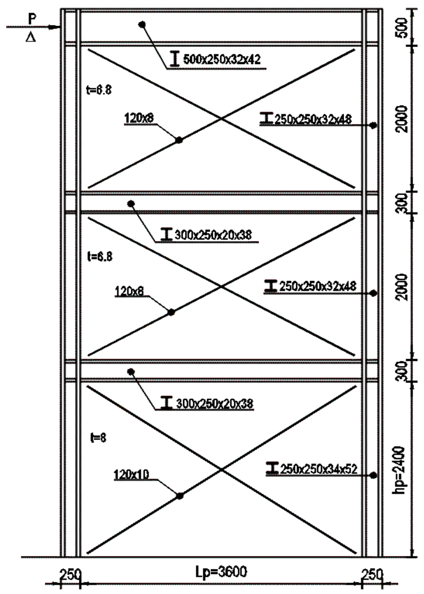

Fig. 10. Dimensional details of the basic model.

IV. PARAMETRIC STUDY

The capacity of steel plate shear walls depends mainly on the stiffness of the edge columns. In this paper, the in-plane stiffness and the area of the edge columns of diagonally stiffened SPSWs are discussed considering various aspect ratio, height-to-thickness ratio, and the number of floors. On the other hand, formulas were proposed to express the in-plane stiffness I_c and the area of the edge columns A_c based on the column flexibility parameter ω_h and the radius of gyration r_x, respectively.

A. Parameters of the column's stiffness on diagonally stiffened steel plate shear walls

Different SPSWs were designated with a range of the number of stories (n=3-7), range of an aspect ratio (L_p/h_p=1-2), and range of height to thickness ratio (λ=200-400) to evaluate the effect of column's in-plane stiffness and area on the shear capacity of SPSWs. The sizes of sections investigated in this study are tabulated in Table II. This parametric study is performed to discuss the influence of varying the thickness, width, and height of the infill panel and the number of floors on the stiffness of the edge columns, and to propose equations to predict the column's in-plane stiffness and area necessary for preliminary design. Table III clarifies the limitations of the parameters considered.

Table- II: Size of sections for parametric analysis.

(a) Section size (L/h=1.0, λ=200)						
ω_h	H (mm)	B (mm)	t_w (mm)	t_f (mm)	r_x* (mm)	I_y/I_x**
3.0	270	270	23	36	108.6	0.42
2.5	320	320	31	46	127.0	0.43
2.1	390	390	35	48	157.0	0.40
1.8	450	450	40	60	181.0	0.42
(b) Section size (L/h=1.0, λ=300)						
ω_h	H (mm)	B (mm)	t_w (mm)	t_f (mm)	r_x* (mm)	I_y/I_x**
3.0	245	245	20	32	99.0	0.42
2.5	290	290	27	41	115.5	0.43
2.1	350	350	32	45	140.4	0.41
1.8	410	410	35	52	165.4	0.41
(c) Section size (L/h=1.0, λ=400)						
ω_h	H (mm)	B (mm)	t_w (mm)	t_f (mm)	r_x* (mm)	I_y/I_x**
3.0	230	230	22	28	92.2	0.40
2.5	270	270	25	38	107.6	0.43
2.1	320	320	31	46	127.0	0.43
1.8	380	380	35	49	152.3	0.41
(d) Section size (L/h=1.5, λ=200)						
ω_h	H (mm)	B (mm)	t_w (mm)	t_f (mm)	r_x* (mm)	I_y/I_x**
3.0	250	250	22	30	100.9	0.40
2.5	290	290	29	43	114.5	0.43
2.1	350	350	35	47	139.1	0.42
1.8	410	410	40	54	163.4	0.41
(e) Section size (L/h=1.5, λ=300)						
ω_h	H (mm)	B (mm)	t_w (mm)	t_f (mm)	r_x* (mm)	I_y/I_x**
3.0	225	225	18	28	91.3	0.41
2.5	265	265	23	37	106.1	0.43
2.1	310	310	29	48	122.5	0.44
1.8	365	365	37	53	144.2	0.43
(f) Section size (L/h=1.5, λ=400)						
ω_h	H (mm)	B (mm)	t_w (mm)	t_f (mm)	r_x* (mm)	I_y/I_x**

3.0	215	215	15	24	88.5	0.40
2.5	250	250	21	32	100.9	0.41
2.1	290	290	29	43	114.5	0.43
1.8	340	340	35	49	134.3	0.43
(g) Section size (L/h=2.0, λ=200)						
ω_h	**H (mm)**	**B (mm)**	t_w **(mm)**	t_f **(mm)**	r_x* **(mm)**	I_y/I_x**
3.0	220	220	25	39	84.7	0.47
2.5	260	260	31	52	98.4	0.49
2.1	310	310	42	60	116.8	0.48
1.8	365	365	42	67	139.9	0.47
(h) Section size (L/h=2.0, λ=300)						
ω_h	**H (mm)**	**B (mm)**	t_w **(mm)**	t_f **(mm)**	r_x* **(mm)**	I_y/I_x**
3.0	200	200	22	34	77.5	0.46
2.5	235	235	28	47	88.9	0.49
2.1	280	280	35	55	105.9	0.49
1.8	325	325	41	67	122.0	0.49
(i) Section size (L/h=2.0, λ=400)						
ω_h	**H (mm)**	**B (mm)**	t_w **(mm)**	t_f **(mm)**	r_x* **(mm)**	I_y/I_x**
3.0	185	180	20	35	70.8	0.46
2.5	220	215	26	44	83.2	0.47
2.1	260	260	31	52	98.4	0.49
1.8	305	300	43	60	114.2	0.47

* in-plane radius of gyration of the column.
**out-of-plane stiffness divided by in-plane stiffness.

Table- III: Description and limitations of the parameters.

Parameter	**Description**	**Limits of parameters**	
		Minimum	**Maximum**
t_p	thickness of infill plate (mm)	4.8	12
L_p	width of infill plate (mm)	2400	6000
h_p	height of infill plate (mm)	1440	3600
n	number of floors	3	7

V. EVALUATION OF PARAMETRIC STUDY RESULTS

Parametric analyses are executed to determine the required economic stiffness of columns. The ranges of ω_h is between 1.8 and 3.0. The shear strength capacity of the wall increases as the column's stiffness increases. The larger the stiffness of the column is, the larger the capacity of the wall is. If columns with small stiffness are used, tension fields are generated, and the system buckles earlier. As a result, a severe decrement and loss in load-carrying capacity and energy dissipation are observed. Fig. 11 illustrates the top displacement plotted against the base shear for n=3, λ=200, 300, and 400 and L_p/h_p = 1,1.5, and 2. In the case of n=3, for ω_h =1.8, 2.1, or 2.5, the greater the drift is, the greater the shear capacity of the wall is. As for the ω_h =3, the shear capacity of the wall decreases as the drift increases, especially for L_p/h_p > 1.5 and λ < 400. For ω_h =2.5, all walls achieved shear strength of more than 95% of the required base shear per AISC [17]. From the results mentioned above, for n=3, the required ω_h could be equal or less than 2.5 so that the wall achieves shear strength, and the column provides sufficient limitation for the development of post-buckling capacity. Therefore, the enlargement of the column's section is unnecessary to assure the development of the tension field for satisfying the requirements of the capacity design.

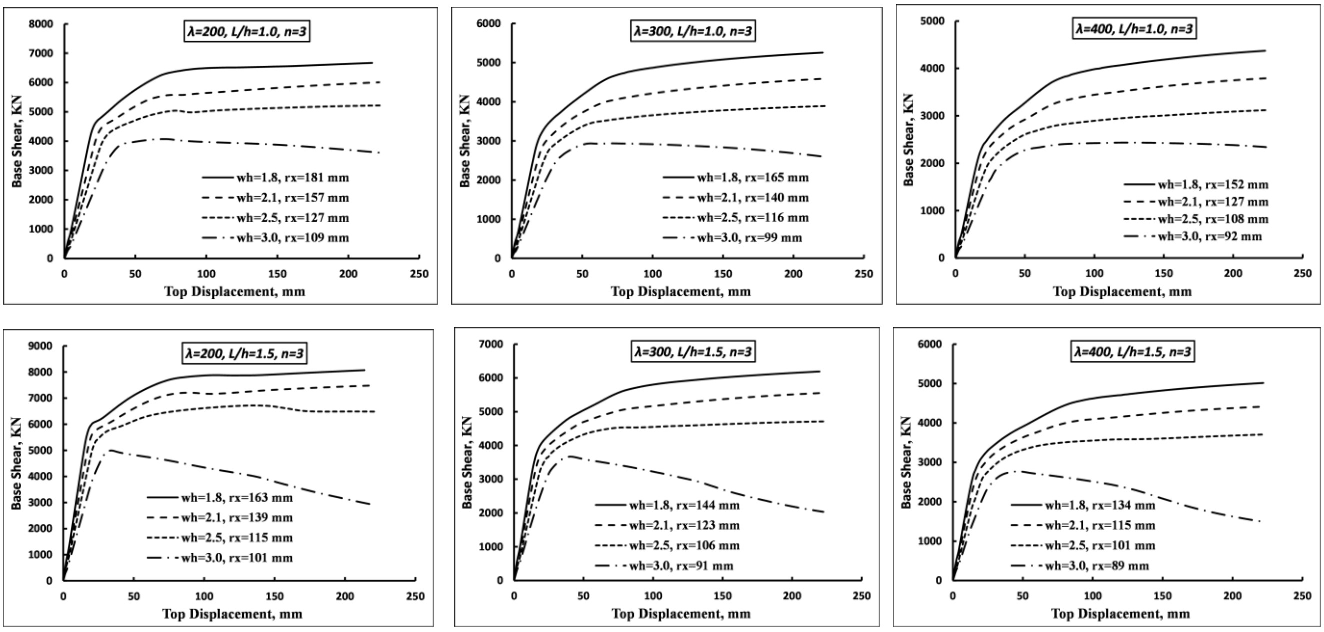

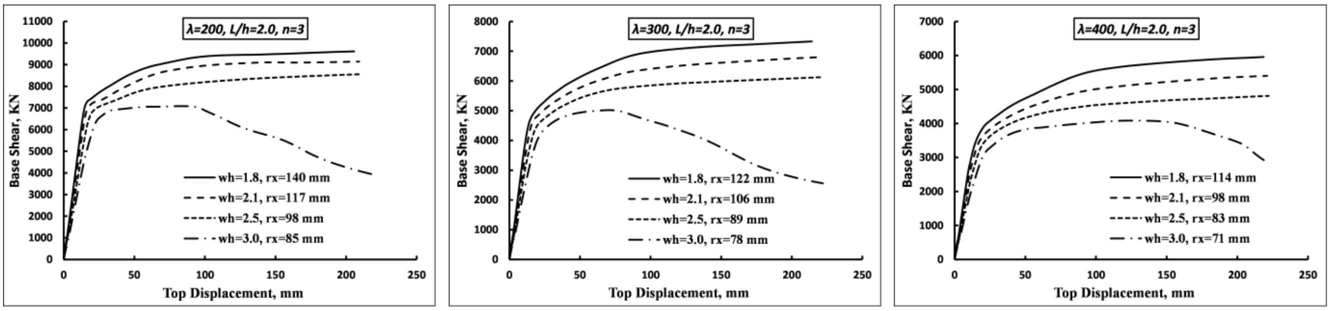

Fig. 11. Base shear and top displacement curves for *n*=3, λ=200, 300 and 400, and L_p/h_p = 1, 1.5, and 2.

Fig. 12 depicts the relation between the top displacement and the base shear for n=7, λ=200, 300, and 400 and L_p/h_p = 1,1.5, and 2. In the case of n=7, for ω_h=1.8, the walls exhibited higher capacity as the drift increases. While for ω_h = 2.1, 2.5, or 3, the walls showed lower capacity as the drift increases. For ω_h=2.1, the walls showed the capacity of almost 80% of the required base shear per AISC [17]. Whereas, for ω_h=1.8, the walls showed a capacity of more than 95%.

Besides the column's in-plane stiffness, the area and out-of-plane stiffness should also be investigated. When columns with a smaller area and smaller out-of-plane stiffness are used, the infill panel of the wall buckle and the system becomes unstable in the out-of-plane direction and starts to fail earlier. Therefore, it is suggested that the columns with out-of-plane stiffness divided by its in-of-plane stiffness could be equal or greater than 0.4.

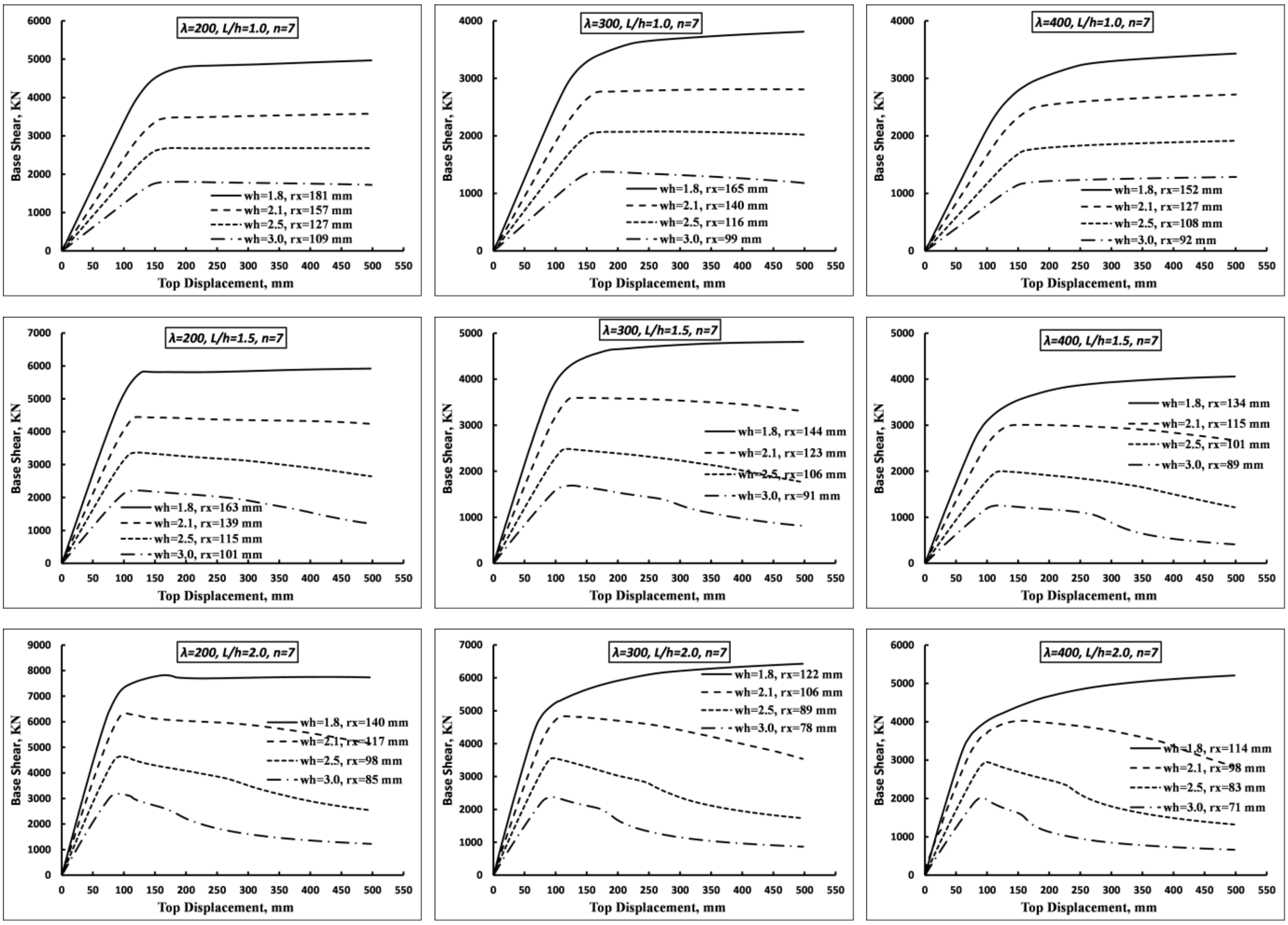

Fig. 12. Base shear and top displacement curves for *n*=7, λ=200, 300 and 400, and L_p/h_p = 1, 1.5, and 2.

Fig. 13 shows the relation between ω_h and the number of stories n for both finite element analysis and the proposed equation. As the number of stories increase, the required ω_h of the column decreases. This is to ensure that the in-fill panel achieves full yield strength. Using the curve fitting method, an equation is proposed to predict the ω_h of the column and expressed as follows:

$$\omega_h = 0.7h\left[\frac{t_i}{2LI_c}\right]^{0.25} * K_h \qquad (3)$$

, where $K_h = 3.4\left(\frac{1}{n}\right)^{0.3}$

Retrieval Number: E2249039520/2020©BEIESP
DOI: 10.35940/ijitee.E2249.039520
Journal Website: www.ijitee.org

Published By:
Blue Eyes Intelligence Engineering
& Sciences Publication

It should be noted that ω_h should be equal or less than 2.5.

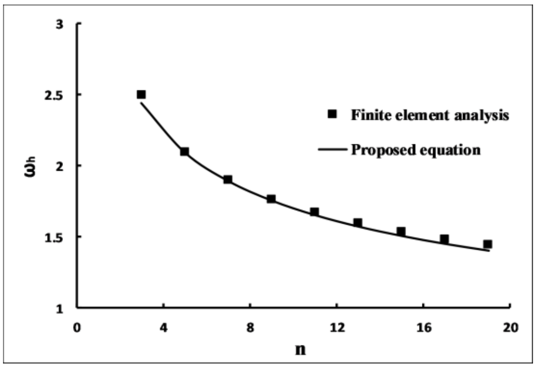

Fig. 13. The relation between ω_h and n.

Excessive finite element analyses were performed to study the influence of varying the infill panel's thickness t_p, length L_p, and height h_p and the number of stories n on the column's in-plane radius of gyration r_x, as characterized in Figs. 14, 15, and 16, respectively. Moreover, Fig. 17 shows the equivalent stresses of different models with variable n, t_p, L_p, and h_p at the final load stage. Based on these results, an equation is proposed to calculate the required r_x of the column, to assure that the web plates don't buckle and the system doesn't fail but remain stable in the out-of-plane direction, and expressed as follows:

$$r_x \le 0.0275 n^{0.3} h_p^{\,1.2} \left(\frac{t_p}{L_p}\right)^{0.25} \tag{4}$$

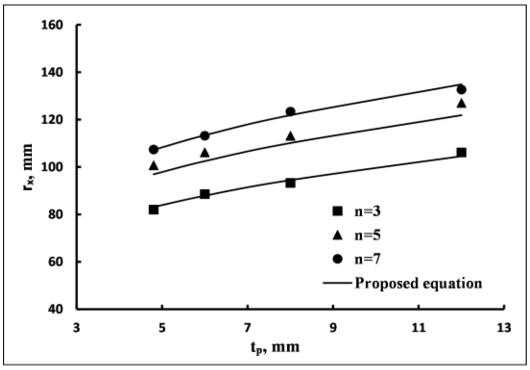

Fig. 14. The relation between the column's in-plane radius of gyration r_x and the thickness of the infill panel t_p.

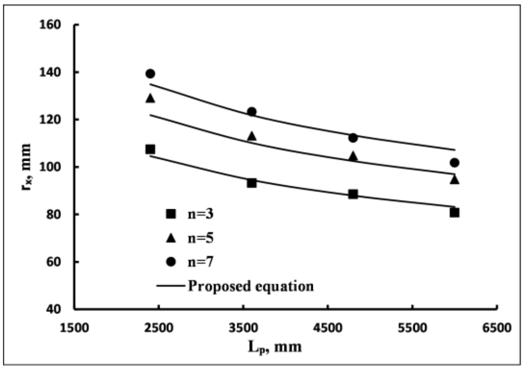

Fig. 15. The relation between the column's in-plane radius of gyration r_x and the length of the infill panel L_p.

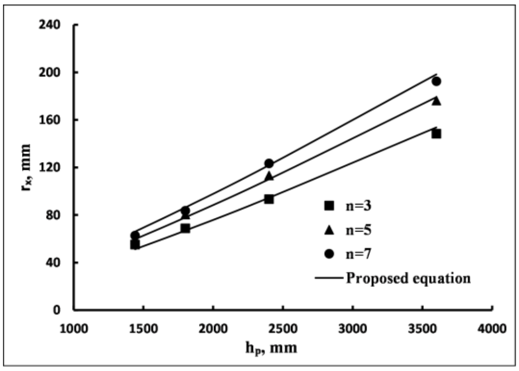

Fig. 16. The relation between the column's in-plane radius of gyration r_x and height of the infill panel h_p.

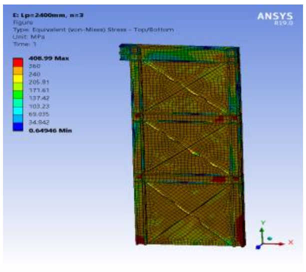

(a) Equivalent stress for *Lp*=2400mm and *n*=3

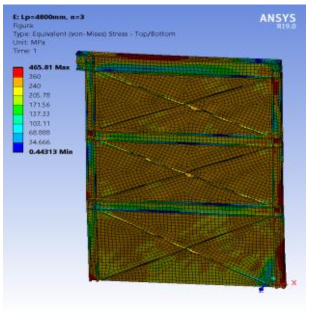

(b) Equivalent stress for *Lp*=4800mm and *n*=3

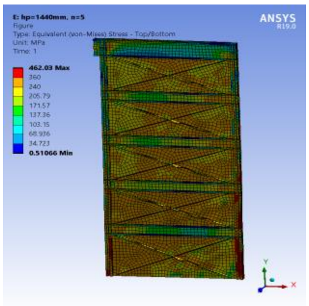

(c) Equivalent stress for *hp*=1440mm and *n*=5

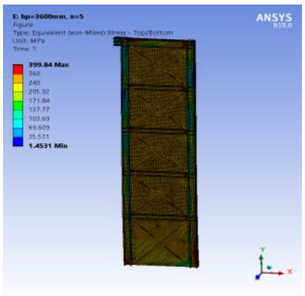

(d) Equivalent stress for *hp*=3600mm and *n*=5

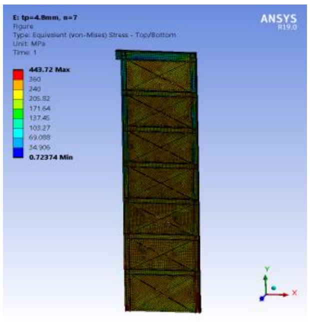

(e) Equivalent stress for *tp*=4.8mm and *n*=7

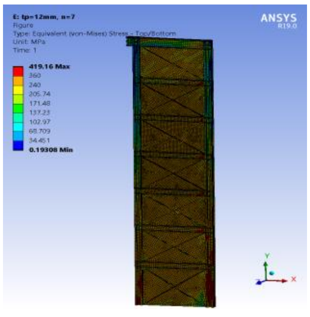

(f) Equivalent stress for *tp*=12mm and *n*=7

Fig. 17. Equivalent stress for different models.

Retrieval Number: E2249039520/2020©BEIESP
DOI: 10.35940/ijitee.E2249.039520
Journal Website: www.ijitee.org

Published By:
Blue Eyes Intelligence Engineering
& Sciences Publication

VI. CONCLUSION

In the current study, parametric analyses are conducted to discuss the influence of varying the thickness, width, and height of the infill panel and the number of floors on the stiffness of the edge columns, and to propose equations to predict the economic column's in-plane stiffness and area necessary for preliminary design. The outcomes indicated that:

- The number of floors (n) has a great influence on the shear capacity of the walls. A greater number of floors lead to buckling in columns and early failure of the system, and therefore increment in the column's rigidity is required.
- The shear capacity of the wall decreases as the drift increases, especially for larger aspect ratio ($L_p/h_p > 1.5$), and smaller height to thickness ratio ($\lambda < 400$).
- The columns' out-of-plane stiffness divided by its in-plane stiffness is suggested to be equal or greater than 0.4.
- Equations are proposed to estimate the required r_x and ω_h of the columns necessary to ensure that the plate achieves full yield strength, and the columns can resist the impact of the tension field.

REFERENCES

1. Caccese, V., Elgaaly, M., and Chen, R. Experimental study of thin steel plate shear walls under cyclic load. *J.Struct. Eng.*, **119**(2), 1993. pp. 573–587.
2. Elgaaly, M., Caccese, V., and Du, C. Post-buckling behavior of steel plate shear walls under cyclic loads. J.Struct. Eng., 119(2), 1993. pp. 588–605.
3. Driver, R. M., Kulak, G. V., Elwi, A. E., and Kennedy, D. J. L. Cyclic tests of four-story steel plate shear wall. J.Struct. Eng., 124(2), 1998. pp. 112–120.
4. Astaneh-Asl, A. Seismic behavior and design of steel plate shear walls. Steel TIPS Rep., Structural Steel Educational Council, Moraga, CA, 2001.
5. Guo YL, Dong QL. Research and application of steel plate shear wall in high-rise buildings. Steel Constr, 25(1), 2005, pp. 1–6.
6. Elbanna AA. Analysis and design of stiffened steel plate shear walls [Ph.D. dissertation]. Cairo University, Faculty of Engineering; 2020.
7. Alinia, M.M., and Dastfan, M. Cyclic behavior, deformability and rigidity of stiffened steel shear panels. J.Constr Steel Res., 63(4), 2007. pp. 554–563.
8. Li, F., Li, H., Li, Z.M., Li, Z.J., Chen, X.F, and Ding, L. Cyclic test of diagonally stiffened steel shear wall. J.Xian Univ. Architect. Technol. (Nat Sci Ed), 41(1), 2009. pp. 57–62.
9. Alavi, E., and Nateghi, F. Experimental study of diagonally stiffened steel shear walls. J.Struct. Eng., 139(11), 2013. pp. 1795–1811.
10. Alavi, E., and Nateghi, F. Experimental study of diagonally stiffened steel shear walls with central perforation. J. Constr. Steel. Res., 89(1), 2013. pp. 9–20.
11. Afshari, M.J., Asghari, A., and Gholhaki, M. Shear strength and stiffness enhancement of cross-stiffened steel plate shear walls. Int. J. Advan. Struct. Eng., 11(1), 2019. pp. 179–193.
12. Omid, H., Ramli Sulong, N.H., and Zainah, I. Cyclic performance of stiffened steel plate shear walls with various configurations of stiffeners. Int. J. Vibroengineering., 20(1), 2018. pp. 459–476.
13. Sigariyazd, M.A., Joghataie, A., and Attari, N.K.A. Analysis and design recommendations for diagonally stiffened steel shear walls. J.Thin-Walled Struc., 103(1), 2016. pp. 72–80.
14. Nateghi, F., and Alavi, E. Non-linear behavior and shear strength of diagonally stiffened steel plate shear walls. IJE Transactions B: Applications., 22(4), 2009. pp. 343–355.
15. Wang, M., Yang, W., Shi, Y., and, Xu, J. Seismic behaviors of steel plate shear wall structures with construction details and materials. J. Constr. Steel. Res., 107(1), 2015. pp. 194–210.
16. Park, HG; Kwack, JH; Jeon, SW; Kim, WK; Choi, IR, Framed Steel Plate Wall Behavior under Cyclic Lateral Loading. ASCE Journal of Structural Engineering, 2007, 133(3), 378-388.
17. American Institute for Steel Construction, ANSI/AISC 341-10 seismic provisions for structure steel buildings, Chicago, IL, USA, 2005.
18. Canadian Standards Associations, CAN/CSA-S16-09, Limit states design of steel structures, Toronto, Canada; 2001.
19. Machaly, E.B., Safar, S.S., and Amer, M.A. Numerical investigation on ultimate shear strength of steel plate shear walls. J.Thin-Walled Struc., 84(1), 2014. pp. 78–90.

AUTHORS PROFILE

Amr A. Elbanna, Assistant lecture, Structural Engineering Department, Faculty of Engineering, Beni-suef University.

Sherif S. Safar, Professor of steel structures and bridges, Structural Engineering Department, Faculty of Engineering, Cairo University.

Mokhtar M. Seddik, Professor of steel structures and bridges, Structural Engineering Department, Faculty of Engineering, Cairo University.